Electroclinic effect in a liquid crystal with chiral nematic and smectic-A phases

J. Etxebarria
Departamento de Física de la Materia Condensada, Facultad de Ciencias, Universidad del País Vasco, Apartado 644, 48080 Bilbao, Spain

J. Zubia
Departamento de Automática, Electrónica y Telecomunicaciones, Escuela Superior de Ingenieros Industriales y de Telecomunicación
Alameda de Urquijo s/n, Universidad del País Vasco, 48013 Bilbao, Spain

(Received 13 March 1991)

The electroclinic effect is studied in a compound that presents a chiral nematic–smectic-A phase sequence. The induced tilt angles are measured as a function of the applied electric fields in both phases. A strong deviation from the linear relationship between the tilt and the applied field is observed, especially in the case of the smectic-A phase. In addition, detailed measurements of the critical behavior of the electroclinic effect at the nematic–smectic-A phase transition are presented. The results are analyzed in the framework of the available theoretical models. Other possible alternatives that could account for the behavior observed at the transition are discussed qualitatively.

PACS number(s): 61.30.−v, 64.70.Md

I. INTRODUCTION

The electroclinic effect was first described by Garoff and Meyer in the smectic-A (Sm-A) phase of the well-known ferroelectric liquid crystal DOBAMBC [1]. It consists in the induction of a molecular tilt when the material is subjected to an electric field perpendicular to the molecular director. Since its discovery, the phenomenon has attracted considerable attention both from fundamental [2–8] and practical [9] points of view. Up to now, most studies of the electroclinic effect have been performed on Sm-A phases of materials built up of chiral molecules, although it is known to take place also in other orthogonal smectic mesophases [10]. However, recently it has been found that the smectic ordering is not essential for the appearance of the electroclinic effect. A tilt in the optical axis proportional to an applied electric field has been observed in a long-pitch chiral nematic (N^*) phase with the helix unwound by surface stabilization [11,12]. The size of the nematic electroclinic effect is quite small and presents a rapid increase on approaching a Sm-A phase. This behavior is very interesting because, in principle, a much slower variation near the N^*–Sm-A transition is theoretically predicted. Since, to the best of our knowledge, this new phenomenon has been investigated in only one compound, it seems of interest to provide more experimental information and compare the new data with the already published results.

In this paper we report on detailed measurements of the electroclinic effect in SCE9, a compound which possesses N^* and Sm-A phases. The electric field effects on the induced tilt have been examined in these two phases. Likewise, the temperature behavior of the effect has been studied near the N^*–Sm-A transition. The results are analyzed in the framework of the available models and other possible alternatives are discussed qualitatively.

II. ORIGIN OF THE NEMATIC ELECTROCLINIC EFFECT

Although a symmetry-based phenomenological model of the nematic electroclinic effect has been given in Refs. [11] and [12], here we offer a simple argument that easily permits one to intuit the phenomenon on a molecular level.

Consider a chiral nematic phase which contains molecules of zigzag shape in such a way that the description of their orientation requires the use of two unit vectors, $\mathbf{n}_1$ (the usual nematic director) and $\mathbf{n}_2$. In this situation, the optical dielectric tensor ϵ_{ij} (or any symmetric second rank tensor) can be expressed to lowest order as

$$\epsilon_{ij}=\epsilon_0\delta_{ij}+\epsilon_1\langle n_{1i}n_{1j}\rangle+\epsilon_2\langle n_{1i}n_{2j}+n_{2i}n_{1j}\rangle+\epsilon_3\langle n_{2i}n_{2j}\rangle \quad (1)$$

where ϵ_0, ϵ_1, ϵ_2, and ϵ_3 are constants. In order to simplify, let us consider that $\mathbf{n}_1$ is perfectly oriented (the nematic order parameter is equal to unity) and $\mathbf{n}_2$ is orthogonal to $\mathbf{n}_1$ so that $\mathbf{n}_1=(0,0,1)$ and $\mathbf{n}_2=(\cos\phi,\sin\phi,0)$ (see Fig. 1). The molecules are supposed to have strong lateral dipoles whose value is given by $\mathbf{d}=\mu\mathbf{n}_1\times\mathbf{n}_2$. If we apply an electric field $\mathbf{E}=(E,0,0)$, the molecules will have an energy $\mathbf{V}=-\mathbf{d}\cdot\mathbf{E}=\mu E\sin\phi$ from which the average values of the different trigonometric functions of ϕ can be calculated. For example, $\langle\sin\phi\rangle$ will be given by

$$\langle\sin\phi\rangle=\frac{\int_0^{2\pi}\sin\phi\exp(-V/kT)d\phi}{\int_0^{2\pi}\exp(-V/kT)d\phi}=-\mu E/2kT \quad (2)$$

assuming the inequality $\mu E\ll 2kT$. Using the above expression for ϵ_{ij} we get

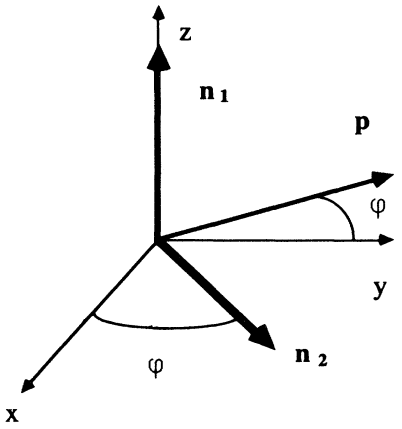

FIG. 1. Schematic description of the orientation of a chiral molecule. $\mathbf{n}_1$ is the usual nematic director and $\mathbf{n}_2$ is a second director orthogonal to $\mathbf{n}_1$, which accounts for the orientation of other transverse molecular parts. The molecule is supposed to have a lateral dipole moment given by $\mathbf{d}=\mu\mathbf{n}_1\times\mathbf{n}_2$.

$$\epsilon=\begin{bmatrix}\epsilon_0+\epsilon_3/2 & 0 & 0\\ 0 & \epsilon_0+\epsilon_3/2 & -\epsilon_2\mu E/2kT\\ 0 & -\epsilon_2\mu E/2kT & \epsilon_1+\epsilon_0\end{bmatrix}. \quad (3)$$

Therefore the presence of the field causes the old principal axes parallel to z and y to rotate at an angle given by $\tan 2\theta=2\epsilon_{32}/(\epsilon_{33}-\epsilon_{22})$, i.e.,

$$\theta=-\epsilon_2/(\epsilon_1-\epsilon_3/2)\mu E/2kT \quad (4)$$

which is linear in the electric field.

III. EXPERIMENT

The compound studied, SCE9, was purchased from BDH Ltd. and used in our experiments without further purification. Above room temperature, the material presents the following phase sequence:

$$I\text{-}(119.5\,^\circ\text{C})\text{-}N^*\text{-}(91.1\,^\circ\text{C})\text{-Sm-}A\text{-}(62.0\,^\circ\text{C})\text{-Sm-}C^*$$

where I represents the isotropic phase. This compound is quite suitable for measuring the nematic electroclinic effect because it presents pitch compensation in the N^* phase and has a negative value of the dielectric anisotrophy.

The sample for our measurements was made of two tin oxide coated glass plates previously treated with nylon 6/6 in order to achieve planar orientation [13]. The material was introduced by capillarity in the isotropic phase and cooled into the N^* phase at 0.1 °C/min. The sample thickness, 4 μm, was determined from the Newton color sequence using a Berek compensator and the birefringence value at room temperature. In the N^* temperature range the helix remained unwound by surface stabilization. This was checked optically with a polarizing microscope. Very good orientation was achieved over the whole sample area (~ 1 cm^2) both at the N^* and Sm-A phases.

The experimental arrangement for measuring the tilt angle was similar to that used in previous works [5,8,11,12]. The light source was a He-Ne laser and the sample was set between crossed polarizers with the angle between the director and first polarizer equal to 22.5°. A sine-wave voltage was applied to the sample and the induced ac light transmission δI was measured with a photodiode and a phase-sensitive detector. Simultaneously, the dc component of the intensity (I_0) was determined with a digital voltmeter. Measurements were performed dynamically at a constant rate of 0.1 °C/min both on heating and cooling and the data were stored every 10 s on a microcomputer. The tilt angle θ was determined by the equation

$$\theta=\delta I/4I_0\ . \quad (5)$$

The experimental resolution in θ was estimated to be better than 10^{-6} rad.

The frequency response of the electroclinic effect was examined for frequencies up to 90 kHz. No relaxational behavior could be found in the N^* phase. The measurements presented below were obtained under an electric field at a fixed frequency of 1 kHz.

IV. ELECTRIC FIELD EFFECT ON THE ELECTROCLINIC BEHAVIOR

The magnitude of the induced tilt angle versus the strength of the applied voltage V is plotted in Fig. 2 at several temperatures in the Sm-A phase. As has been found before [4,7,14,15], θ shows a nonlinear behavior near the Sm-A–Sm-C^* transition temperature T_{AC}. It is worth noticing, however, that the nonlinearities found here are stronger than those reported previously. The observed behavior can be explained in terms of a simple

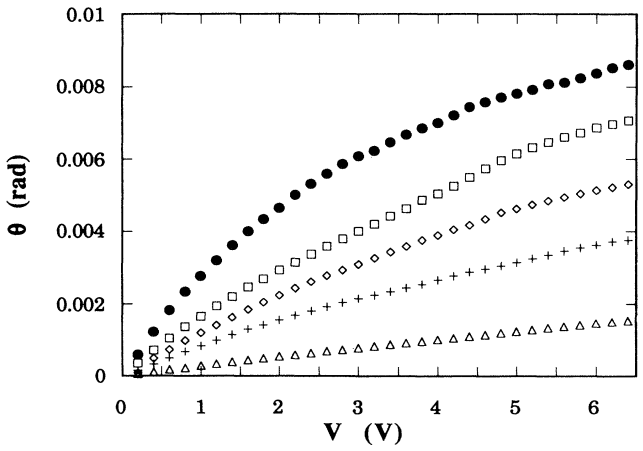

FIG. 2. Induced tilt angle as a function of the applied voltage in the Sm-A phase. The five curves correspond to the following temperatures: $T=62.5$, 63.0, 63.5, 64.0, and 67.0 °C. A strong nonlinear behavior near the Sm-A–Sm-C^* transition can be observed.

mean-field model [14,15] with a θ^4 term in the free-energy expansion around T_{AC}. The model predicts a field dependence $\theta \propto E^x$ with $x=1$ for sufficiently low fields and $x=\frac{1}{3}$ in the high-field limit. The deviation from linearity is more appreciable close to T_{AC}, where the θ^4 contribution to the free energy becomes more important. Figure 3 shows the field dependence of the effective exponent x for the curves obtained at $T=62.5$, 63, and 67 °C. The exponent was obtained from the derivative of a least-squares fit of $\log_{10}\theta$ versus $\log_{10}V$. The results are in accordance with the expectations. Data scatter somewhat in the limit of low fields but the effective exponent is close to unity in that region. As the temperature approaches T_{AC}, x takes lower values for high voltages. Finally, for the curve at 62.5 °C, 0.5 °C above the Sm-A–Sm-C^* transition, the crossover to the $x=\frac{1}{3}$ regime is almost complete.

Figure 4 shows the effect of the field in the Sm-A phase near T_{NA}. For low fields θ behaves almost linearly but presents an anomalous decrease above a certain threshold. This phenomenon can be explained as due to a shift in the T_{NA} temperature to lower values with increasing fields. This fact was confirmed by means of direct microscopic observation. The texture change, which is quite slight, takes place at lower temperatures when the field goes up and, as can be seen in Fig. 5, T_{NA} follows approximately a quadratic law in the applied voltage.

It is worth pointing out here that the electric field is not completely responsible for the observed T_{NA} shift. The shift is, at least in part, due to the heating of the sample by the Joule effect and, therefore, T_{NA} must be considered as an effective transition temperature. Assuming a typical specific heat $C_p \sim 1$ J/g K, we have checked that, in this temperature region in which the material is rather fluid, the resistivity is small enough so as to explain at least half the shift detected. Likewise, the quadratic law in the applied voltage can be accounted for within this hypothesis, since the temperature rise is proportional to V^2.

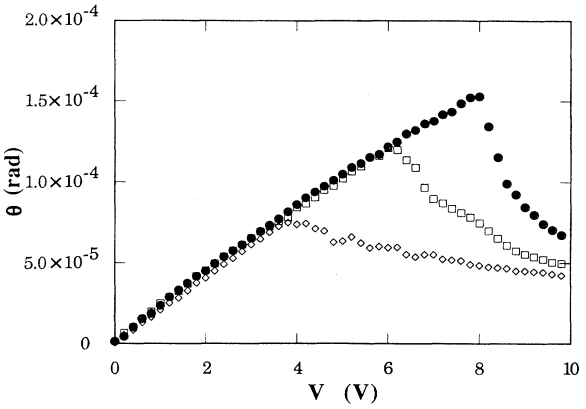

FIG. 4. Induced tilt angle as a function of the applied voltage around the N^*–Sm-A transition. The decreasing behavior above a certain threshold is due to the electric field dependence of T_{NA}. The circle, square, and tilted square symbols represent $T=90.6$, 90.8, and 91.0 °C, respectively.

The nonlinear relationship between the tilt angle and the electric field was also observed in the N^* phase. Figure 6 gives some examples of such a behavior. As the field is increased, the tilt angle begins to deviate in a qualitatively similar way to that found for the Sm-A phase near T_{AC}. Also in analogy to that case, the deviation is stronger for temperatures close to T_{NA}. An evolution of this type can be obtained within the usual linear approach if the shift of the effective transition temperature with the field is taken into account. As has been pointed out before, T_{NA} decreases for increasing fields. Therefore the application of an electric field produces an enlargement of the distance from each temperature to the actual transition point, which tends to decrease the θ value. The greater nonlinearity near the N^*–Sm-A transition can also be explained in terms of the sharpness of the temperature dependence of θ near T_{NA} (see next section).

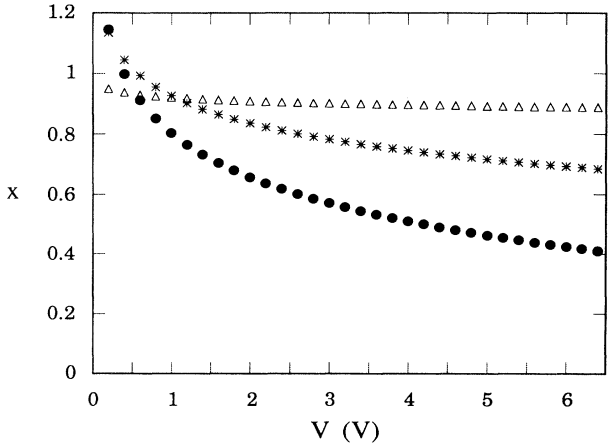

FIG. 3. Voltage dependence of the exponent x of the applied field. The circle, asterisk, and triangle symbols represent $T=62.5$, 63, and 67 °C, respectively.

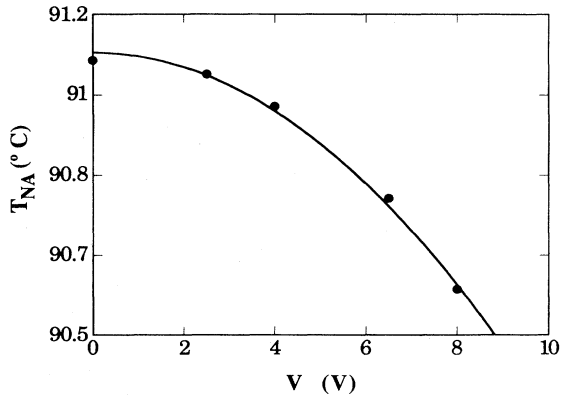

FIG. 5. Voltage dependence of the effective temperature of the N^*–Sm-A phase transition. The continuous line is the best fit to a quadratic law, $T_{NA}(V)-T_{NA}(0) \propto V^2$.

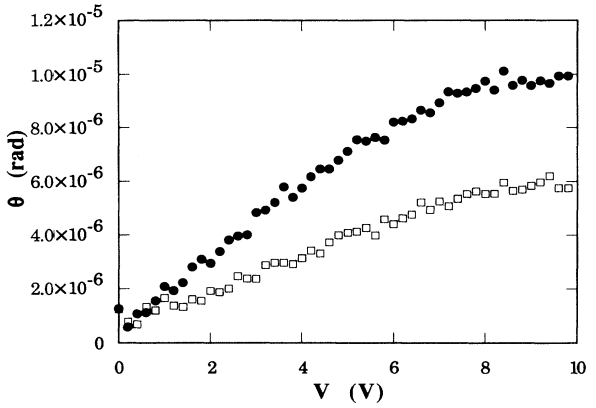

FIG. 6. Induced tilt angle as a function of the applied voltage in the N^* phase. The circle and square symbols refer to $T=94.0$ and 96.0 °C, respectively.

V. THE ELECTROCLINIC EFFECT AT THE N^*–Sm-A TRANSITION

Figure 7 shows the temperature dependence of the induced tilt angle θ for an applied voltage of 2.5 V. As can be seen, θ takes a small value in the N^* phase which increases slightly when the temperature is lowered and presents a strong pretransitional effect in the vicinity of the N^*–Sm-A transition point. A similar behavior has been reported by Li, Petschek, and Rosenblatt [11] in their original article about the nematic electroclinic effect. However, some minor differences can be noted in our data, such as the appearance of a small but conspicuous peak near the N^*–Sm-A transition, which is absent in the results published so far [11,12]. In these works, a theoretical model was proposed for the nematic electroclinic effect which implies that near the N^*–Sm-A transition temperature T_{NA}, the temperature behavior for θ should be proportional to the square of the smectic order parameter. However, due to the sharpness of the effect

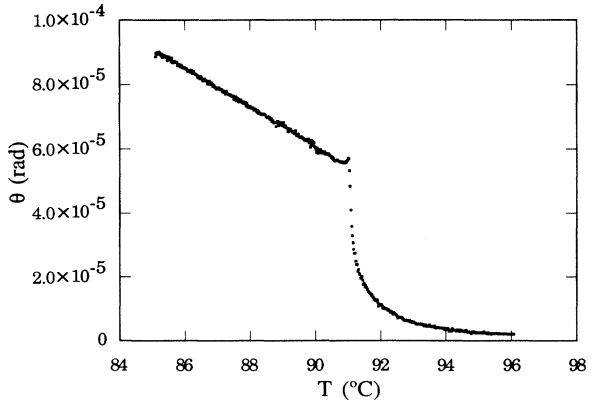

FIG. 7. Temperature dependence of the tilt angle induced by a sine-wave voltage of 2.5 V and 1 kHz around the N^*–Sm-A phase transition.

near T_{NA}, no good correspondence was found with the experimental results.

In order to test our data with these theoretical predictions, the results near T_{NA} were analyzed in terms of the expression

$$\theta = At^{1-\alpha} + Bt + \theta_0 \tag{6}$$

where A and B are constants, α is the critical exponent for the specific heat, $t=(T-T_{NA})/T_{NA}$ is the reduced temperature, and θ_0 is the value of the tilt angle at $t=0$. The stability of the least-squares fits of our data to Eq. (6) was tested by range shrinking and three temperature ranges were used, range I: $t<10^{-3}$; range II: $t<3\times10^{-3}$; range III: $t<10^{-2}$.

Since according to Eq. (6) $d\theta/dt$ is extreme (or diverges) for $t=0$, T_{NA} was taken at the point in which the slope of the $\theta(T)$ curve is maximum ($T=91.07$ °C). In each range, two different fits were performed. In the first one (1) the linear term was omitted and in the second one (2) the parameter B was freely adjustable. In all cases θ_0 was held fixed at its experimental value at T_{NA}. The least-square α values and the χ^2 values for the fits are given in Table I.

As can be seen, the fits are not bad in general and a certain improvement in their quality is obtained by allowing $B\neq0$. This is especially the case of range III, in which fit 2 provides a substantial improvement. However, it should be noted that there does not exist any correspondence between the α values obtained from fits 1 and 2 even within the same temperature range. This indicates a lack of reliability in the resulting values of α. Moreover, there is a clear and systematic trend in the α value obtained in both sets of fits as the range is varied and no convergence is achieved in any of them. Figure 8 offers an explanation for this fact. The temperature dependence of $\theta_0-\theta$ for $t>0$ is shown in a logarithmic scale. Since the slope of this curve is a measure of $1-\alpha$ and, as can be seen, it seems to vary continuously without reaching a converging limit value at the phase transition, it is understandable that Eq. (6) cannot account for the data. On the other hand, the range in which the critical exponents obtained vary seems to be quite unrealistic for a material with a MacMillan ratio T_{NA}/T_{IN} as low as 0.928. In these cases, specific-heat measurements can usually be fitted successfully according to the 3D–XY model in which $\alpha=-0.007$ [16,17].

Regarding the region $t<0$, it is even more evident that,

TABLE I. Results of the least-squares fits of the induced tilt angle above the N^*–Sm-A transition using Eq. (6). χ^2 was defined as $\chi^2=(1/N)\sum_i[\theta(t_i)-\theta_i]^2/\sigma_i^2$, where N is the number of data points and σ_i the standard deviation, which was set to 5×10^{-7} for all points.

	Range					
	I		II		III	
Fit	α	χ^2	α	χ^2	α	χ^2
1	0.61	1.7	0.68	2.0	0.78	6.8
2	0.35	1.1	0.54	0.8	0.65	1.0

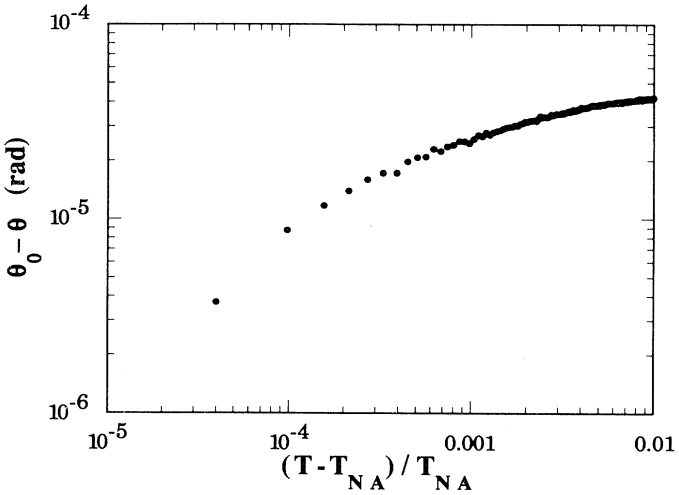

FIG. 8. Log-log plot of the tilt angle relative to its value at T_{NA} vs the reduced temperature above the N^*–Sm-A transition.

due to the presence of the small peak in our tilt data, Eq. (6) (changing t by $|t|$) cannot explain the observed θ behavior in a reasonable temperature range. Therefore, as was found in Ref. [12], the conclusion is reached that the induced tilt angle at the N^*–Sm-A transition cannot be described as a quantity proportional to the square of the smectic order parameter.

At this point it is interesting to ask why the electroclinic effect increases so abruptly at the N^*–Sm-A transition. The electroclinic effect in the N^* phase has been explained as due to the biasing of the rotation of the molecules around their long axes (originated by an electric field perpendicular to the director), without involving a physical tilt of the molecules. If the optical dielectric tensor of a molecule is not codiagonal with its inertial tensor the molecular rotational hindrance provokes the appearance of an optical tilt. It is clear that this mechanism can give rise to an electroclinic effect both in the N^* and Sm-A phases. In the Sm-A case, however, the appearance of the smectic layers can permit the existence of another contribution to the electroclinic effect. This second mechanism involves the physical tilt of the molecule (or the molecular director $\mathbf{n}_1$) with respect to the layer normal. The layer normal provides now a reference direction which allows one to distinguish between the untilted and tilted configurations. As a direct consequence of this second mechanism, the electroclinic effect would imply a lowering of the smectic layer thickness. Such a contraction, however, seems to be quite unfavorable from the energetic point of view and, probably, in order to avoid it, the layers should deform. Some authors have experimentally observed in the Sm-A phase a distortion of the smectic layers as a consequence of the electroclinic effect. An undulation of the planes, similar to what happens in the Helfrich-Hurault effect [18] has been proposed [19,20]. Some recent x-ray results [21] suggest the bending or tilting of the layer structure with a distortion similar to the chevron formation in the Sm-C^* phases. Nevertheless, the mechanism as well as the structure of the deformation remains unknown at the moment. Anyway, a process of this type could start at the N^* phase near the transition, where smectic cybotactic groups begin to develop. Likewise, this mechanism should involve the elastic constants which, as is well known, show strong pretransitional effects at the N^*–Sm-A transition and, therefore, could explain the anomalous behavior found for the electroclinic effect.

The rubbing direction as a conceptually different axis from the nematic director can also be used to explain the sharp change of the observed effect at the N^*–Sm-A transition. According to Ref. [22], both in the N^* as in the Sm-A phases, there exists the possibility of surface contributions to the free energy of chiral nature of the form

$$\delta F_s = \int_S dS\, K_c(\mathbf{s}\cdot\mathbf{n})[\mathbf{s}\cdot(\mathbf{E}\times\mathbf{n})] \tag{7}$$

where δF_s is the surface free-energy contribution, dS is the surface element, K_c a constant dependent on the surface, $\mathbf{s}$ a unit vector along the rubbing direction, $\mathbf{n}$ the molecular director, and $\mathbf{E}$ the electric field. The above term can be written as

$$\delta F_s = -SK_cE\theta(0) \tag{8}$$

for small tilts $\theta(0)$ of the surface molecules with respect to the rubbing axis. If in the absence of field the surface energy takes the form [23]

$$F_s = \tfrac{1}{2}SK_s\theta(0)^2 \tag{9}$$

[where K_s is a positive constant, thus favoring $\theta(0)=0$], the additional term δF_s produces a tilt on the surface molecules $\theta(0)=K_c/K_sE$, which is linear in the electric field. The rotation of the alignment at the surface can then give rise to a nonzero tilt value along the whole sample thickness, whose instantaneous deformation profile upon the application of an ac field will depend, among other things, on the magnitude of the twist elastic constant K_2 of the material. As K_2 diverges at the N^*–Sm-A transition, the temperature behavior of the optical signal might be quite abrupt, as experimentally observed.

Evidently, this treatment of the problem is completely different from the explanation given above. According to this approach, the observed phenomenon is considered as a surface flexoelectric effect of chiral nature [22] rather than a bulk electroclinic effect. These is, however, a serious drawback in considering the effect as a surface effect. The problem is that, in this hypothesis, the order of magnitude of the response time should be slower than is experimentally observed. Taking a typical viscosity $\eta\sim 0.1$ poise and $K_2\sim 10^{-6}$ dyn, the relaxation time $\tau\sim\eta d^2/(\pi^2K_2)$ turns out to be about 10^{-3} s for our $d=4$ μm sample. This would imply a relaxation frequency about two orders of magnitude smaller than the upper limit we have examined. As has been mentioned before, no such relaxational behavior has been detected.

Evidently, an increase of K_2 by a factor of 100 near T_{NA} could, in principle, shift the relaxation frequency towards values high enough so as not to be in contradiction

with the rapid response of the effect. Such an increase does not seem to be very likely but, in order to fully disregard this surface flexoelectric approach, it would be worth examining the magnitude of the elastic constants near T_{NA} in this material.

Note added in proof. During the proof correction of this paper we became aware of another work on the nematic electroclinic effect by L. Komitov *et al.* [Ferroelectrics **114**, 167 (1991)].

ACKNOWLEDGEMENT

This work is supported by the CICYT (Comisión Interministerial de Ciencia y Tecnología) of Spain under project No. MAT88- 0324-CO2-02.

[1] S. Garoff and R. B. Meyer, Phys. Rev. Lett. **38**, 848 (1977). DOBAMBC stands for *p*-(*n*-decyloxybenzylidene)-*p*-amino-(2-methyl-butyl)cinnamate.

[2] G. Andersson, I. Dahl, P. Keller, W. Kuczynski, S. T. Lagerwall, K. Skarp, and B. Stebler, Appl. Phys. Lett. **51**, 640 (1987).

[3] Ch. Bahr and G. Heppke, Liq. Cryst. **2**, 825 (1987).

[4] S. Nishiyama, Y. Ouchi, H. Takezoe, and A. Fukuda, Jpn. J. Appl. Phys. **26**, L1787 (1987).

[5] R. Qiu, J. T. Ho, and S. K. Hark, Phys. Rev. A **38**, 1653 (1988).

[6] Z. Li and C. Rosenblatt, Phys. Rev. A **39**, 1594 (1989).

[7] J. Etxebarria, A. Remón, M.J. Tello, and J. L. Serrano, Liq. Cryst. **4**, 543, (1989).

[8] J. A. M. M. van Haaren and G. L. J. A. Rikken, Phys. Rev. A **40**, 5476 (1989).

[9] G. Andersson, I. Dahl, L. Komitov, S. T. Lagerwall, K, Skarp, and B. Stebler, J. Appl. Phys. **66**, 4983 (1989).

[10] Ch. Bahr and G. Heppke, Phys. Rev. A **37**, 3179 (1988).

[11] Z. Li, R. G. Petschek, and C. Rosenblatt, Phys. Rev. Lett. **62**, 769 (1989); **62**, 1577(E) (1989).

[12] Z. Li, A. D. Lisi, R. G. Petschek, and C. Rosenblatt, Phys. Rev. A **41**, 1997 (1990).

[13] J. S. Patel, T. M. Leslie, and J. W. Goodby, Ferroelectric **59**, 137 (1984).

[14] S. D. Lee and J. S. Patel, Appl. Phys. Lett **54**, 1653 (1989).

[15] S. D. Lee and J. S. Patel, Appl. Phys. Lett **55**, 122 (1989).

[16] C. W. Garland, G. Nounesis, K. J. Stine, and G. Heppke, J. Phys. (Paris) **50**, 2291 (1989).

[17] G. Nounesis, C. W. Garland, and R. Shashidhar, Phys. Rev. A **43**, 1849 (1991).

[18] P. G. de Gennes, *The Physics of Liquid Crystals* (Clarendon, Oxford, 1974), pp. 289–292.

[19] J. Pavel and M. Glogarova, Ferroelectrics **114**, 131 (1991)

[20] J. Pavel and M. Glogarova, Liq. Cryst. **9**, 87 (1991).

[21] M. Johno D. L. Chandani, Y. Takanishi, Y. Ouchi, H. Takezoe, and A. Fukuda, Ferroelectrics **114**, 123 (1991).

[22] I. Dahl, Ph. D. thesis, Chalmers University of Technology, Goteborg, 1990.

[23] P. G. de Gennes, *The Physics of Liquid Crystals* (Clarendon, Oxford, 1974), pp. 74–76.